Bio-Inspired Glucose Control in Diabetes Based on an Analogue Implementation of a β-Cell Model

Ilias Pagkalos, Pau Herrero, Christofer Toumazou, *Fellow, IEEE*, and Pantelis Georgiou, *Senior Member, IEEE*

***Abstract*—This paper presents a bio-inspired method for *in-vivo* control of blood glucose based on a model of the pancreatic β-cell. The proposed model is shown to be implementable using low-power analogue integrated circuits in CMOS, realizing a biologically faithful implementation which captures all the behaviours seen in physiology. This is then shown to be capable of glucose control using an *in silico* population of diabetic subjects achieving 93% of the time in tight glycemic target (i.e., [70, 140] mg/dl). The proposed controller is then compared with a commonly used external physiological insulin delivery (ePID) controller for glucose control. Results confirm equivalent, or superior, performance in comparison with ePID. The system has been designed in a commercially available 0.35 μm CMOS process and achieves an overall power consumption of 1.907 mW.**

***Index Terms*—Analogue, artificial pancreas, bio-inspired, diabetes, glucose control, insulin delivery, log-domain.**

I. Introduction

DIABETES Mellitus is one of the most rapidly growing chronic diseases in modern society affecting 3–5% of the total population on earth. It is normally characterized by an increase in blood glucose which occurs either because the pancreas does not produce enough insulin or because the produced insulin is not functional. Type 1 diabetes mellitus (T1DM), which amounts to 10% of the diabetic population is an autoimmune condition which results in complete destruction of insulin secreting β-cells of the pancreas leaving the body unable to control its blood glucose. If left unmanaged, it can have long term side effects such as blindness, kidney failure and heart disease.

Current treatment of T1DM involves insulin injection after meals using an insulin pen or an insulin pump. Although this works in the short term, subjects T1DM still spend a large amount of time with high-blood glucose, or hyperglycaemia putting them at risk. The Diabetes Control and Complications Trial [1] demonstrated that intensive insulin management reduced complications by as much as 50–76%. The potential benefits of having an automated system to control blood glucose has lead to the development of the Artificial Pancreas.

Manuscript received August 31, 2013; revised December 08, 2013; accepted January 12, 2014. Date of publication March 26, 2014; date of current version May 23, 2014. This work was supported by The Wellcome Trust. This paper was recommended by Associate Editor K.-T. Tang.

I. Pagkalos is with the Department of Bionengineering, Imperial College London, SW7 2AZ, U.K. (e-mail: ilias.pagkalos@imperial.ac.uk).

P. Herrero, C. Toumazou, and P. Georgiou are with the Department of Electrical and Electronic Engineering, Centre of Bio-Inspired Technology, Institute of Biomedical Engineering, Imperial College London, SW7 2AZ, U.K. (e-mail: pherrero@imperial.ac.uk; c.toumazou@imperial.ac.uk; pantelis@imperial.ac.uk).

Color versions of one or more of the figures in this paper are available online at http://ieeexplore.ieee.org.

Digital Object Identifier 10.1109/TBCAS.2014.2301377

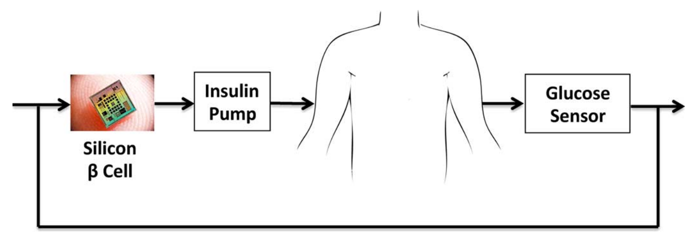

Fig. 1. Bio-inspired glucose control using the silicon β-cell.

The Artificial Pancreas is a closed-loop system whose main role is replicate the function of a healthy human pancreas to improve control of glyceamia [2] shown in Fig. 1. It normally comprises of:

- A continuous blood glucose sensor which is connected to the body either subcutaneously or intravascularly.
- An insulin pump that delivers insulin either subcutaneously or intravenously.
- A device which runs a control algorithm to relate the rate of delivering insulin with blood glucose level.

The Biostator was one of the first artificial pancreas systems introduced 40 years ago [3]. Due to its intravenous nature, it was only used in the clinic by the patient bedside and was very useful in a wide range of medical studies such as assessment of the influence of drugs on health, on measurement insulin resistance using clamp techniques, and treatment assessment on surgical interventions. Since the initial creation of the Biostator there has been an evolution in portable subcutaneous continuous glucose monitoring (CGM) [4] and insulin pump technologies [5], allowing subjects with diabetes to manage their blood glucose outside the hospital environment in an open-loop fashion. These are still sub-optimal however, with subjects still spending a large amount of time with high blood glucose levels. As a result there have been several attempts to create an artificial pancreas all working with existing subcutaneous glucose sensors and insulin pumps [2], [6]. These, however, have to accommodate for delays of insulin absorption in the subcutaneous space and inaccuracies of glucose measurements making there adoption challenging [7]. More recently, we have seen the advent of peritoneal insulin pumps [8], [9] and rapid acting insulin alternatives [10] which would potentially allow faster control of blood glucose with minimal delay. Furthermore, CGM technology is continuously improving [11] and new promising solutions are emerging [12].

Key to the realisation of an artificial pancreas is an electronic device which can bridge the glucose sensor and insulin pump and offer full closed-loop control. This should ideally replicate the behaviour of the β-cells of the pancreas to be able to mimic insulin secretion. Additionally, it should be miniature to allow complete integration in a portable medical device. This can be facilitated by implementation on a CMOS microchip [13], [14].

Towards this goal, we present a bio-inspired method for treatment of T1DM, through an analogue implementation of the insulin secreting pancreatic β-cell. We show its design using low-power integrated circuits in CMOS and follow on to show how this bio-inspired method can be used to control a FDA-accepted [15] virtual T1DM diabetic population comprising of 10 adults and 10 adolescents. Finally, we present a comparison between the bio-inspired approach and a commonly used blood glucose control technique.

This paper is organized as follows. Section II describes the mathematical model of the β-cell which is used for our bio-inspired approach. Section III illustrates the analogue implementation and the analysis of each block of the system. Section IV presents the results of the circuit showing that it achieves comparable responses as observed in β-cells. Finally Section V shows how this controls blood glucose in a type-1 diabetic population and how this compares to a conventional method of control. We conclude with a discussion on the benefits of our approach.

II. The β-Cell Model

The idea of using a physiological approach for blood glucose control was first postulated by Steil and colleagues [16]. In this work, a minimal model of insulin secretion, proposed earlier by Breda and colleagues,[17] was used for blood glucose control. This simple model represents the insulin secretion by decomposing it into a static rate of secretion, which basically depends on the plasma glucose concentration (second phase), and a dynamic secretion rate, which depends on the rate of change of plasma glucose concentration (first phase). Steil and colleagues [16] compared the minimal model of insulin secretion with a PID controller, the behaviour of which also exhibits biphasic response, and concluded that both were able to fit experimental data. However, the insulin secretion model was less stable than the PID controller under closed-loop conditions due to the simplification of the β-cell model.

More recent developments of mathematical models of β-cell physiology, [18]–[21] which are able to describe the glucose-induced insulin release at a molecular level, have opened the door to a new class of bio-inspired glucose control algorithms. Initial minimal models of insulin secretion such as the ones proposed in Hovorka and colleagues,[22] Toffolo and colleagues,[23] Cretti and colleagues,[24] Mari and colleagues,[25] and Breda and colleagues [17] are not able to represent some of the experimental data, probably because of their excessively simplistic structure. On the other hand, more sophisticated models such as the ones proposed by Pederson and colleagues, [18] Bertuzzi and colleagues,[19] and Chen and colleagues, [20] can be difficult to implement in a closed-loop controller because of their high number of parameters and equations.

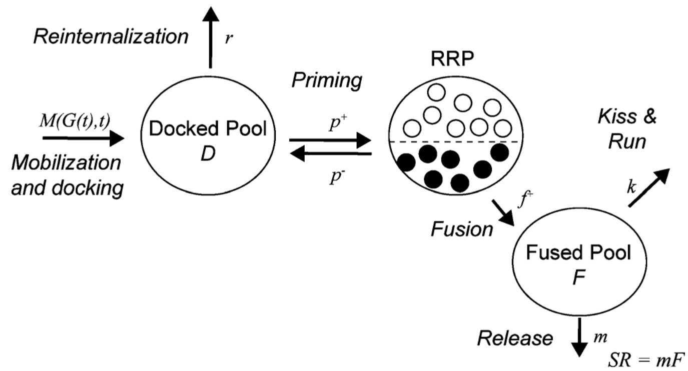

Fig. 2. Overview of the β-cell model [21], the RRP is divided into granules located in silent cells (o) and granules located into triggered cells (●). (Reprinted with permission of the Royal Society.)

In 2008, a mathematical model for the granular release of insulin was reported [21] which is now being used as control algorithm for the Bio-inspired Artificial Pancreas (BiAP) [6]. This model is able to represent most of the experimental data, including the biphasic response of insulin secretion, the staircase modulation of insulin secretion, the potentiation effect of glucose, and the kiss-and-run effect of insulin secretion granules. Furthermore, its relative simplicity makes it convenient for practical closed-loop control implementation.

Fig. 2 shows an overview of the model. In particular, the model introduces mobilization of secretory granules from a reserve pool to the cell periphery, where they attach to the plasma membrane (i.e., docking). The granules can mature further (i.e., priming), thus entering the readily releasable pool (RRP). The possibility of so-called *kiss-and-run* exocytosis is included, where the fusion pore reseals before the granule cargo is released. The model assumes that the beta cells have different glucose thresholds for triggering Ca^{2+}. Additionally the model assumes that a proportion of the cells remains silent and the remaining cells release insulin depending on the glucose value. This can be described by a density function given by

$$\Phi(G) = \int_0^G \phi(g)\,\mathrm{d}g \tag{1}$$

where G is the current value of glucose and ϕ is a time-independent function and represents the proportion of triggered cells for each glucose value. The values for ϕ change when the value of basal glucose changes. For the evaluated scenarios of this work, the value for basal glucose was set at 100 mg/dl.

Mobilisation of the cells depends on the value of glucose with a delay of τ and is described by

$$\frac{dM(G,t)}{dt} = \frac{M_\infty(G) - M(G,t)}{\tau} \tag{2}$$

where $M_\infty(G)$ is the expression for the steady-state mobilisation and its response is a sigmoidal function (Hill equation) given by

$$M_\infty(G) = \frac{c \cdot G^{nM}}{(K_{mM})^{nM} + G^{nM}} + M_0 \tag{3}$$

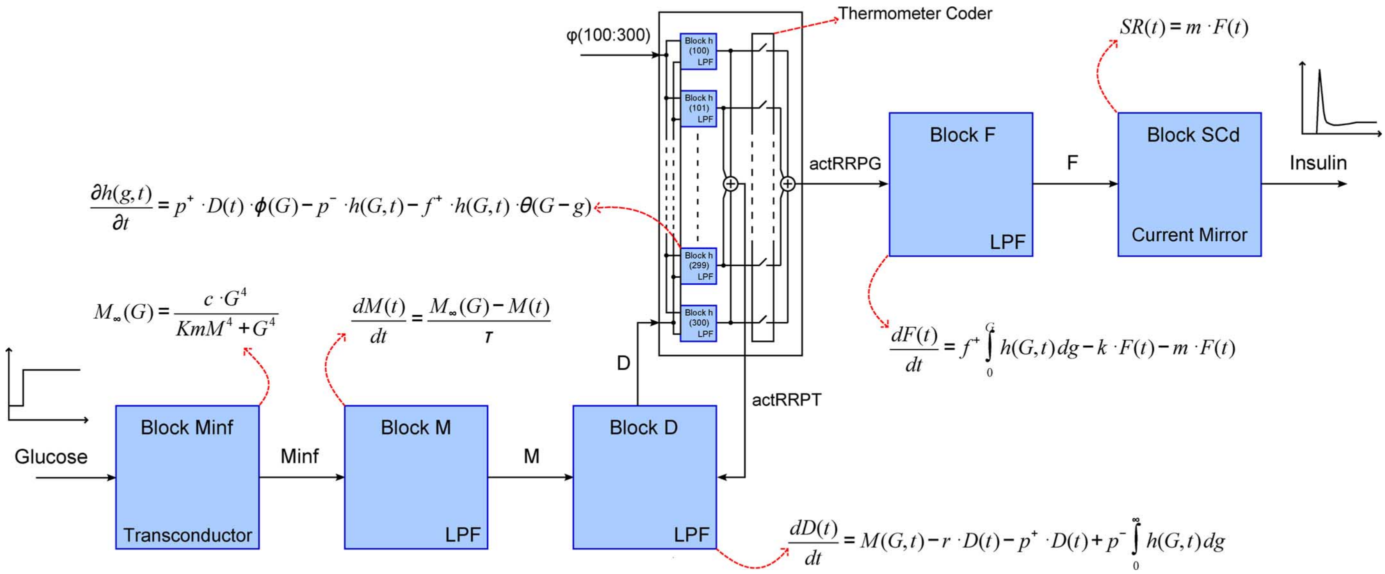

Fig. 3. Block diagram of the system, the glucose input in mV drives the M_∞ transconductor and then the signal as current passes through block M and D to form the input for the block which computes the approximations of the integral terms of (4) and (7) as $actRRPT$ and $actRRPG$, respectively. Then $actRRPG$ drives block F, a low pass filter whose output multiplied by m produces the insulin output in current.

where nM is the Hill coefficient, K_{mM} is the apparent dissociation constant of the Hill equation, M_0 is the basal mobilisation rate and c is the maximal rate of stimulated mobilisation. The docked pool equation is given by

$$\frac{dD(t)}{dt} = M(G,t) - r \cdot D(t) - p^+ \cdot D(t) + p^- \int_0^\infty h(g,t)\,\mathrm{d}g \tag{4}$$

where r is the rate of reinternalisation, $h(g,t)$ is a time-varying density function which indicates the amount of insulin in the RRP. Triggered granules are fused with a rate of f^+, hence we have

$$\frac{\partial h(g,t)}{\partial t} = p^+ \cdot D(t) \cdot \phi(g) - p^- \cdot h(g,t) - f^+ \cdot h(g,t) \cdot \theta(G-g) \tag{5}$$

where p^+ and p^- are the rates for priming and depriming of the granules, respectively. The function $\theta(G-g)$ is the Heaviside unit step function which returns 1 if the input is greater than zero and 0 if the input is smaller than zero. The insulin secretion rate is given by

$$SR(t) = m \cdot F(t) + SR_b \tag{6}$$

where SR_b is the basal insulin secretion (not shown in Fig. 2), m is a rate constant and F is the fused pool described as

$$\frac{dF(t)}{dt} = f^+ \int_0^G h(g,t)\,\mathrm{d}g - k \cdot F(t) - m \cdot F(t) \tag{7}$$

where k is a rate constant called *kiss-and-run*. More details for the model can be found at [21].

III. An Analogue Implementation

This work presents an analogue implementation of the β-cell model proposed by [21]. This circuit is an electronic realisation of the original β-cell model equations which is achieved with the use of several blocks shown in Fig. 3. This includes a transconductor to replicate the steady state mobilisation, followed by several low pass filters to implement time-dependant terms and then a block controlled by a thermometer coder in such a way to produce the approximations of integral terms of the model's dynamics. The output of this block finally drives another low pass filter and after a scaling with the use of a current mirror the final output of the system is produced representing the proposed amount of insulin.

The glucose input of the model, with a typical range of glucose levels variations from 0 to 500 mg/dl, is mapped as the voltage input of the circuit with a range of 0 – 500 mV and drives the transconductor which mimics the response of M_∞ ((3)). Then, the signal is processed as indicated by the block diagram of the circuit presented in Fig. 3, and ends up producing an output in the range of 0–6 nA corresponding to real insulin secretion values of 0–60 $\mu\mathrm{g/min}$. We now proceed to explain how each function in the model was realized.

A. M_∞ Transconductor

In order to replicate the function of M_∞ as described in (3), the block M_∞ would require adders, multipliers and dividers. Due to the complexity of building an electronic circuit to replicate the function of M_∞, another method to achieve the same output was adopted. In particular, the response of M_∞ to an input glucose sweeping from 0 to 500 mg/dl, is a sigmoidal function [Fig. 4(b), red line].This sigmoidal function can be replicated by an area scaled differential pair transconductor. Fig. 4(a) shows the topology, in which two differential pairs with scaled transistor sizes (ratio 6:1 outer to inner) are being used in order to achieve the aiming linearity of M_∞. The achieved sigmoidal

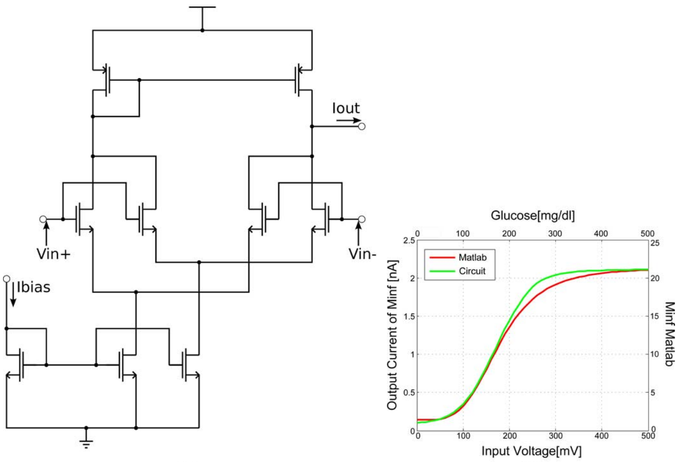

(a) (b)

Fig. 4. Transconductor, in (b) the red line is the response of M_∞ from Matlab and the green line the approximated M_∞ response from the circuit. (a) Topology. (b) Circuit/Matlab Response.

function [Fig. 4(b), green line] presents a small error rate, compared to the desired response (red line). The impact of this error rate to the final output of the system was negligible.

B. Bernoulli Cell Formalism for Low Pass Filters

The realisation of the model's time-dependant dynamics was performed with the use of the Bernouli Cell (BC) formalism [26] to implement log-domain filters. The BC and its non-linear aspect (NBC) [27] can produce the solution of linear and non-linear differential equations (DE) of the form

$$nCV_T\dot{w}(t) + a(t)\cdot w(t) = u(t), \tag{8}$$

where $w(t)$ is the state variable, $u(t)$ is the input, $a(t)$ is a coefficient of the DE, n is the subthreshold slope, C is the value of the capacitor and V_T is the thermal voltage. The first order DE of β-cell model are using constant in time coefficients and since the state variables can be represented by currents as $w(t) = I_{OUT}(t)/I_Q$ the electronic equivalent of (8) is

$$\begin{aligned} nCV_T\frac{\dot{I}_{OUT}(t)}{I_Q} + I_A\frac{I_{OUT}(t)}{I_Q} &= I_{IN}(t) \Rightarrow \\ \dot{I}_{OUT}(t) + \frac{I_A}{nCV_T}I_{OUT}(t) &= \frac{I_Q}{nCV_T}I_{IN}(t). \end{aligned} \tag{9}$$

This equation describes the function of circuit shown in Fig. 5, where I_{OUT} is the output current, I_{IN} is the input current, the ratios I_A/nCV_T and I_Q/nCV_T represent the coefficients of the DE and I_A and I_Q are biasing currents. The current sources I_K are being used for biasing purposes and are placed in such a way in order to satisfy the translinear loop and not affect the DE. The dynamics of β-cell model described by (2), (4), (5), (7) can be represented in the form of (9) as follows:

$$\begin{aligned} Eq.(2) &\Rightarrow \tau\dot{M}(t) + M(t) = M_\infty \\ &\Rightarrow \dot{I}_M + 0.0667\cdot I_M = 0.0667\cdot I_{M_\infty}, \end{aligned} \tag{10}$$

$$\begin{aligned} Eq.(4) &\Rightarrow \dot{D}(t) + (r+p^+)D(t) \\ &= M(G,t) + p^-\cdot actRRPT \\ &\Rightarrow \dot{I}_D + 0.038\cdot I_D = I_M + 0.1\cdot actRRPT, \end{aligned} \tag{11}$$

$$\begin{aligned} Eq.(7) &\Rightarrow \dot{F}(t) + (k+m)F(t) = f^+ actRRPG \\ &\Rightarrow \dot{I}_F + 1.09\cdot I_F = 6.2\cdot actRRPG, \end{aligned} \tag{12}$$

$$\begin{aligned} Eq.(5)(\theta=0) &\Rightarrow h(\dot{G},t) + p^- h(G,t) = p^+ D(t)\phi(G) \\ &\Rightarrow \dot{I}_{h_0} + 0.1\cdot I_{h_0} = 0.03\cdot I_D\cdot I_{\phi(G)}, \end{aligned} \tag{13}$$

$$\begin{aligned} Eq.(5)(\theta=1) &\Rightarrow h(\dot{G},t) + (p^- + f^+)h(G,t) = p^+ D(t)\phi(G) \\ &\Rightarrow \dot{I}_{h_1} + 6.3\cdot I_{h_1} = 0.03\cdot I_D\cdot I_{\phi(G)} \end{aligned} \tag{14}$$

where actRRPT and actRRPG are the approximations of the integral terms of (4) and (7) expressed as $actRRPT = \sum_{k=0}^{\infty} h(k,t)$ and $actRRPG = \sum_{k=0}^{G} h(k,t)$. The values of the parameters were taken from [21]. Table I summarizes the biasing currents and the values of the capacitors for every block describing the equations above. All the filters used are 1st order log-domain low-pass filters with a 20 db/decade attenuation realizing the same dynamics of (9). The circuit of Fig. 5 has been used to implement these with cutoff frequency (f_o) and parameters summarized in Table I. Moreover large devices ($W/L = 100\ \mu\mathrm{m}/10\ \mu\mathrm{m}$) have been used for all transistors to ensure good matching and reliable translinear operation and currents have been chosen to be below 100 nA to guarantee weak-inversion operation.

C. Thermometer Coder

$actRRPG$ and $actRRPT$ are the inputs of the subsystems block F and block D, respectively shown in Fig. 3. $actRRPT$ is the sum of all outputs of h blocks and since are currents the sum of them can be easily extracted by driving them all to the same node. $actRRPG$ is the sum of outputs of h blocks whose glucose thresholds are lower than the glucose input of the system. Thus a thermometer coder to control the state of the switches ("open", input higher than glucose threshold, "close" input lower than glucose threshold) was used to drive the desired currents in the same node in order to compute the value of $actRRPG$. The same technique is used for the selection of either block $h0$ or $h1$, the former is used for glucose input values higher than the glucose threshold while the latter for values lower than the threshold.

Ideally since the range of glucose is from 0 mg/dl to 500 mg/dl and the sensitivity is 1 mg/dl, a number of 500 comparators and pairs of h blocks were required. However, because the non-zero values of ϕ are only 200 (corresponding for glucose values from 100 mg/dl to 300 mg/dl), this number was decreased to 200.

As can be seen in Fig. 6, the thermometer coder consists of 200 comparators where each of them compares the input voltage (the input glucose of the system) with a different threshold voltage. This different threshold voltage replicates the different glucose threshold for every h block. This implies that depending on the input voltage, the output of the comparators that have a threshold voltage lower than the input voltage will be one (closed switch), while the ones with a threshold

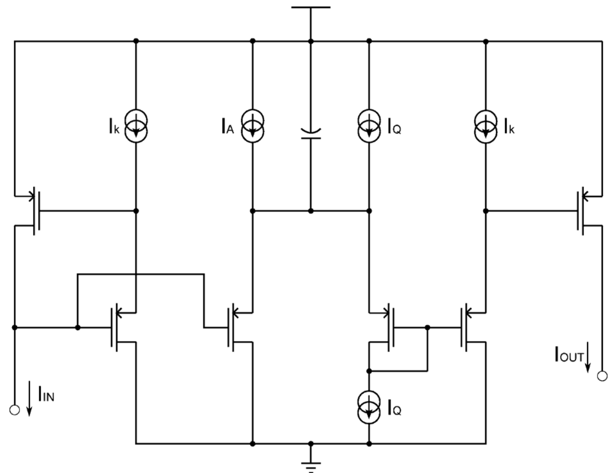

Fig. 5. First order log-domain circuit as proposed in [27].

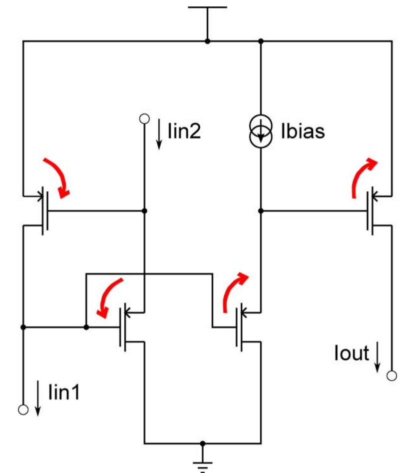

Fig. 7. Translinear multiplier topology.

TABLE I
SPECIFICATIONS FOR THE BERNOULLI CELL CIRCUITS

		$I_A(A)$	$I_Q(A)$	$Capacitor(F)$	f_o(Hz)	$Gain$
Block M		100p	100p	45n	10 m	1
Block D		380p	10n	300n	6m	26.31
Block F		1.76n	10n	48n	173.5m	5.68
Block h	h0	340p	100p	100n	15.9m	0.3
	h1	20.8n	100p	100n	1	0.0048

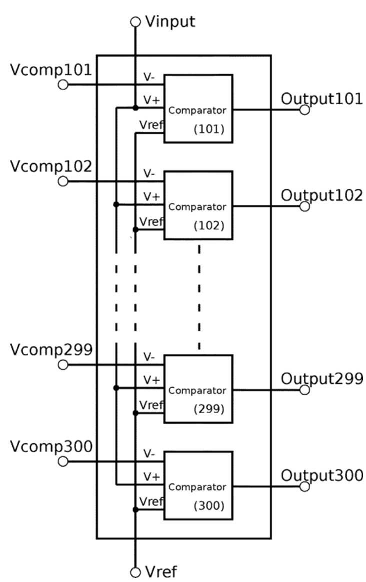

Fig. 6. Thermometer Coder. The variables $\mathrm{Vcomp101}, \mathrm{Vcomp102}, \ldots, \mathrm{Vcomp300}$ represent the values of different voltage threshold for each comparator.

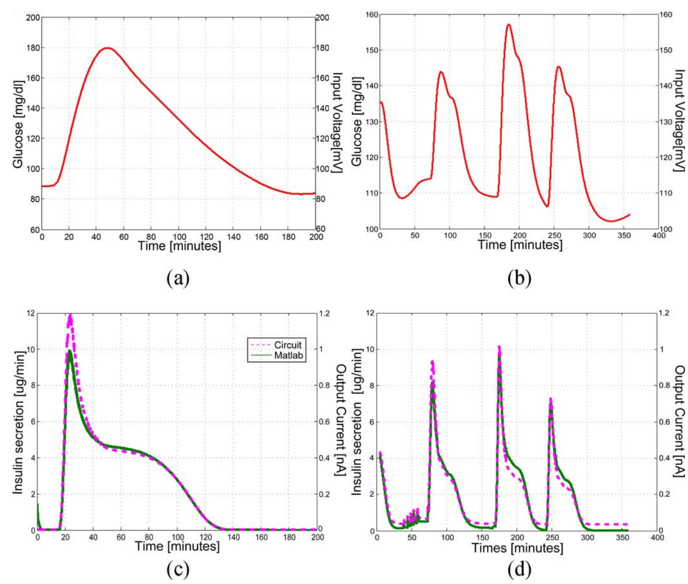

Fig. 8. Glucose inputs for 1 meal and 3 meals scenarios (upper graphs). Corresponding insulin secretion responses by Matlab and circuit implementation (lower graphs). Green solid line corresponsds to Matlab simlulation and the magenta dashed line to the circuit simulation. (a) Glucose Input (1 meal). (b) Glucose Input (3 meals). (c) Insulin Secretion (1 meal). (d) Insulin Secretion (3 meals).

voltage higher than the input voltage will be zero (opened switch).

D. Multiplier

A multiplier was designed to perform the internal computations between the main blocks of the system. Most of the internal computations were multiplications, between an input and a constant parameter. For that reason a current mirror with scaled transistor sizes was preferred instead of a translinear multiplier. However, a translinear multiplier cell was designed in order to apply the multiplication of D and ϕ. The result of this multiplication is the input of block h. In this occasion a current mirror is not possible to be used, since D is an internal variable signal and ϕ is an input of the system.

Fig. 7 shows the translinear multiplier cell. The red arrows in Fig. 7 indicate the transilinear loop which is described by (15).

$$I_{in1} \cdot I_{in2} = I_{bias} \cdot I_{out} \Rightarrow I_{out} = \frac{I_{in1} \cdot I_{in2}}{I_{bias}} \tag{15}$$

I_{bias} scales down the product of the multiplication by factor of 1 nA.

IV. CIRCUIT RESULTS

The circuit was designed in the commercially available 0.35 $\mu\mathrm{m}$ CMOS technology with an operating power supply

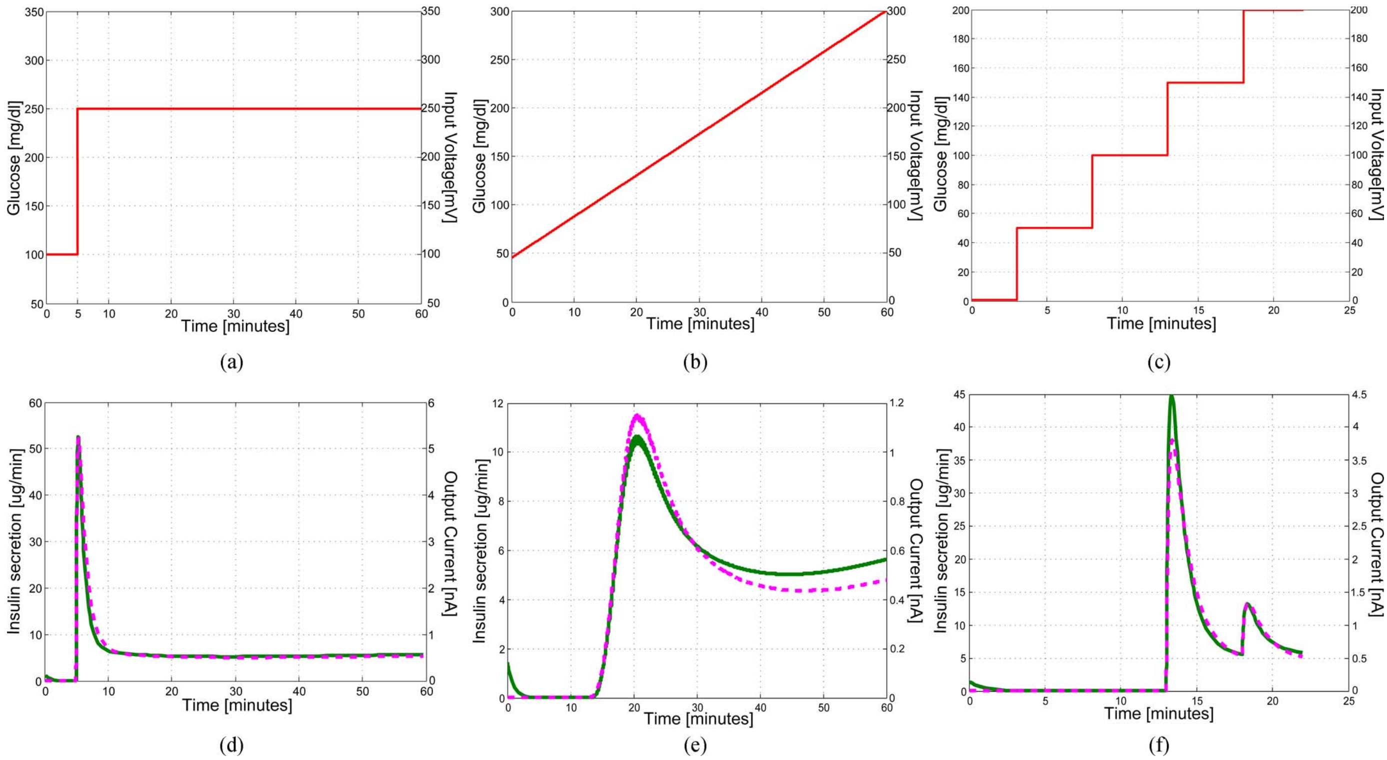

Fig. 9. Insulin secretion responses by Matlab and circuit implementation (lower graphs) to different glucose inputs (upper graphs). Green solid line corresponds to Matlab simulation and magenta dashed line to the circuit simulation. (a) Glucose input for step scenario. (b) Glucose input for ramp scenario. (c) Glucose input for staircase scenario. (d) Insulin secretion for step scenario. (e) Insulin secretion for ramp scenario. (f) Insulin secretion for staircase scenario.

of 3.3 V. Each pair of sub-figures in Fig. 9 illustrates the input glucose on the top figure and the insulin secretion on the bottom. We tested the circuit to show that it accurately replicates behaviours exhibited by real β-cells [21]. The input conditions for the four scenarios that were tested are :

- Step Scenario [Fig. 9(a)] : A step in glucose levels at $\mathrm{t} = 5\ \mathrm{min}$ from $\mathrm{G} = 100$ to $250\ \mathrm{mg/dl}$
- Slow Ramp Scenario [Fig. 9(b)] : The value of glucose linearly increases with a slow rate, starting from 45 mg/dl at 0 seconds to 300 mg/dl at 60 seconds.
- Staircase Scenario [Fig. 9(c)] : The glucose starts from 0 mg/dl for the first 3 minutes and constantly increases by 50 mg/dl every 5 minutes until time reaches 18 minutes where the glucose stabilizes at 200 mg/dl for the last 3 minutes.
- Meal Scenario [(Fig. 8(a)] : The input glucose is taken from a real meal scenario as proposed in [21].
- 3 Meals Scenario [Fig. 8(b)]: A computer simulation environment [15] was used to simulate a typical glucose response of a T1DM subject to a meal scenario consisting of 3 meals (i.e., breakfast, lunch, dinner) containing 40 g, 60 g and 50 g of carbohydrates, respectively.

On the insulin secretion figures, the green solid line represents the response from Matlab and the magenta dashed line the result from the circuit. These results demonstrate the close matching of the circuit responses with the corresponding ones from Matlab. The minor mismatch at the output of the circuit is the result of the switching performance for the creation of $actRRPG$. A minor delay which exists between the switching states (open-close) causes a distortion to the response. In Fig. 8(d), it is worth noting the close matching of the response from Matlab and the response from the circuit implementation, with a mean error of $0.0871\ ug/\mathrm{min}$.

TABLE II
DETAILED POWER CONSUMPTION OF THE SYSTEM

Power Consumption	
Comparator	9.35 uW
Thermometer Coder	1.85 mW
Multiplier	42.9nW
Block h	20 nW
Block F	2 nW
Block M	6.78 nW
Block D	13.3 nW
Block M_{inf}	17.025 nW
Overall	1.907 mW

Table II summarizes the measured power consumption of each block of the circuit. Despite the circuit complexity the power consumption has remained reasonably low due to sub-threshold operation. The bottleneck of the circuit's power consumption lies with the number of comparators required in the thermometer coder, which can be replaced with a more power efficient solution.

V. COMPARISON WITH *e*PID CONTROLLER

To test the performance of the β-cell model as a bio-inspired artificial pancreas controller (BIAP), a comparison with the ePID controller proposed by Medtronic (Northridge, CA, USA) [7] was carried out. To carry out such comparison, the FDA-accepted UVa-Padova T1DM simulator [15] was employed. In particular, the 10 adult and 10 adolescent virtual populations form the simulator were selected. The 10 paediatric subjects available in the UVa simulator have extreme glucose dynamics, and in-line with other studies have not been considered here [28], [29].The simulator was configured to sense blood glucose intravascularly and to deliver insulin intravenously. Although the intravenous route is not practical in an ambulatory setting (e.g., cannula occlusions), the advent of new insulin delivery routes [8], [9], rapid acting insulin alternatives [10] and CGM technologies [12], make this assumption not that unrealistic.

Since the glucose sensing and insulin delivery route was selected, the *insulin feedback* term in the ePID controller, which is designed to compensate delays due to the subcutaneous route, was not required. Therefore, the equations representing the employed ePID controller are

$$PID(k) = P(k) + I(k) + D(k), \quad (16)$$

$$P(k) = K_p \cdot [G(k) - G_{sp}], \quad (17)$$

$$I(k) = I(k-1) + \frac{Kp}{T_I} \cdot [G(k) - G_{sp}], \quad (18)$$

$$D(k) = K_p \cdot T_D \cdot dGdt(k) \quad (19)$$

where P, I, and D denote the proportional, integral, and derivative terms of the PID algorithm; G denotes sensor glucose; G_{sp} is the glucose set point; $dGdt$ denotes the rate of change of G; and Kp, TD and TI are tuning parameters. $I(0)$ was set to the basal insulin delivery (I_b) and its range was constrained by

$$I(k) = \min(I(k), I_{\max 1}) \text{ if } G(k) > G_R, \quad (20)$$

$$I(k) = \min(I(k), I_{\max 2}) \text{ otherwise} \quad (21)$$

where $I_{\max 1} = 3 \cdot I_b$, $I_{\max 2} = K_p \cdot (G_{sp} - G_R)$ and $G_R = 60 \text{ mg/dL}$. It is worth noting that these constraints may allow insulin delivery in the hypoglycemic range if glucose concentration is increasing rapidly.

Since the β-cell model [21] employed in the bio-inspired controller does not incorporate basal insulin suppression at low blood glucose concentration levels, this effect was incorporated as follows:

$$SR = K \cdot m \cdot F + K_b \cdot SR_b \quad (22)$$

where K is tuneable gain for patient individualisation and K_b is a variable gain defined as

$$K_b = \frac{G - G_H}{G_{sp} - G_H} \quad (23)$$

being $G_H = 70 \text{ mg/dL}$ and K_b constrained between $[0, 1]$. The patient individualization in the analogue implementation is easily achieved using a digitally programmable current mirror at the output, which receives a binary value of the parameter K and then scales the output $m \cdot F$ to $K \cdot m \cdot F$ as in (22).

Standard metrics provided by the UVa-Padova T1DM simulator, such as mean blood glucose (mean BG), risk index (RI), percentage of time in target ($BG \in [70, 140] \text{ mg/dL}$), percentage of time above target ($BG > 140 \text{ mg/dL}$) and percentage of time below target ($BG < 70 \text{ mg/dL}$), were employed for comparison purposes. It is important to note that the

TABLE III
COMPARISON BETWEEN BIAP AND ePID FOR 10 ADULTS. (A) 10 ADULTS WITH BIAP. (B) 10 ADULTS WITH ePID

(a)

Adult	mean BG mg/dl	RI –	BG∈[70,140] % time	B>140 % time	BG<70 % time
1	99	1.28	0.98	0.013	0
2	109	0.27	1	0	0
3	107	0.55	0.98	0.010	0
4	107	0.72	0.93	0.062	0
5	103	0.72	1	0	0
6	104	0.47	1	0	0
7	111	0.31	1	0	0
8	109	0.31	1	0	0
9	122	0.99	0.84	0.152	0
10	102	1.12	0.97	0.027	0
Mean	107	0.68	0.973	0.026	0

(b)

Adult	mean BG mg/dl	RI –	BG∈[70,140] % time	B>140 % time	BG<70 % time
1	99	1.25	0.98	0.013	0
2	102	0.55	1	0	0
3	102	0.73	0.99	0.007	0
4	105	0.90	0.93	0.066	0
5	102	0.67	1	0	0
6	103	0.57	1	0	0
7	104	0.50	1	0	0
8	105	0.48	1	0	0
9	128	1.27	0.67	0.323	0
10	123	1.40	0.76	0.233	0
Mean	107	0.84	0.935	0.064	0

TABLE IV
COMPARISON BETWEEN BIAP AND ePID FOR 10 ADOLESCENTS. (A) 10 ADOLESCENTS WITH BIAP. (B) 10 ADOLESCENTS WITH ePID

(a)

Adolescent	mean BG mg/dl	RI –	BG∈[70,140] % time	B>140 % time	BG<70 % time
1	107	0.27	0.99	0.007	0
2	154	6.40	0.49	0.503	0
3	103	0.69	0.98	0.010	0
4	103	0.82	0.96	0.034	0
5	104	0.79	0.95	0.045	0
6	108	0.84	0.94	0.059	0
7	129	3.44	0.74	0.256	0
8	118	1.92	0.82	0.177	0
9	103	0.64	0.98	0.010	0
10	107	0.43	1	0	0
Mean	114	1.62	0.89	0.110	0

(b)

Adolescent	mean BG mg/dl	RI –	BG∈[70,140] % time	B>140 % time	BG<70 % time
1	106	0.33	0.98	0.010	0
2	155	5.67	0.46	0.534	0
3	102	0.84	0.98	0.017	0
4	5.69	0.99	0.95	0.045	0
5	102	1.38	0.96	0.034	0
6	5.88	1.00	0.93	0.066	0
7	106	5.71	0.56	0.430	0
8	133	3.30	0.70	0.298	0
9	102	0.85	0.98	0.013	0
10	100	0.90	1	0	0
Mean	116	2.10	0.85	0.145	0

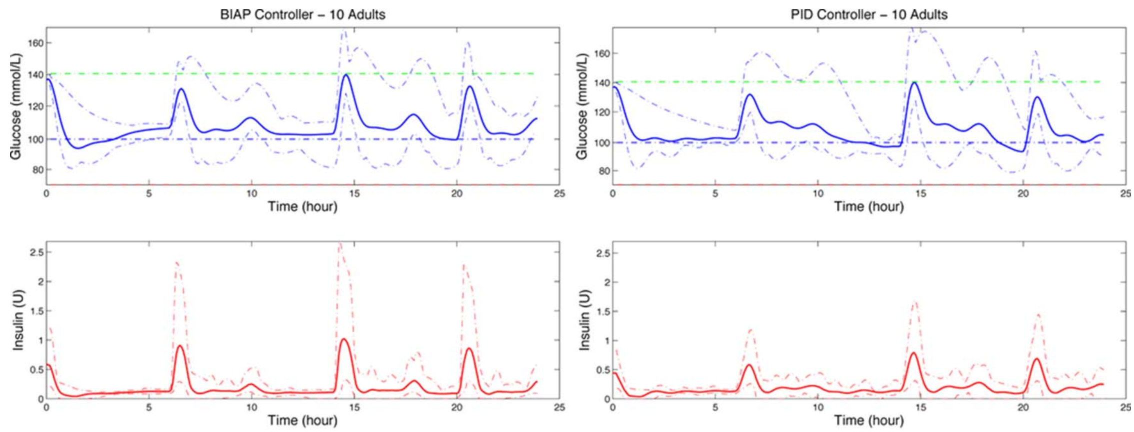

(a) (b)

Fig. 10. ePID vs. BIAP in 10 adults. Solid lines represents mean glucose concentration and mean insulin delivery. Dashed lines represent the envelopes containing all the curves. Breakfast, lunch and dinner occur at 6, 14 and 21 hour, respectively. (a) BIAP. (b) ePID.

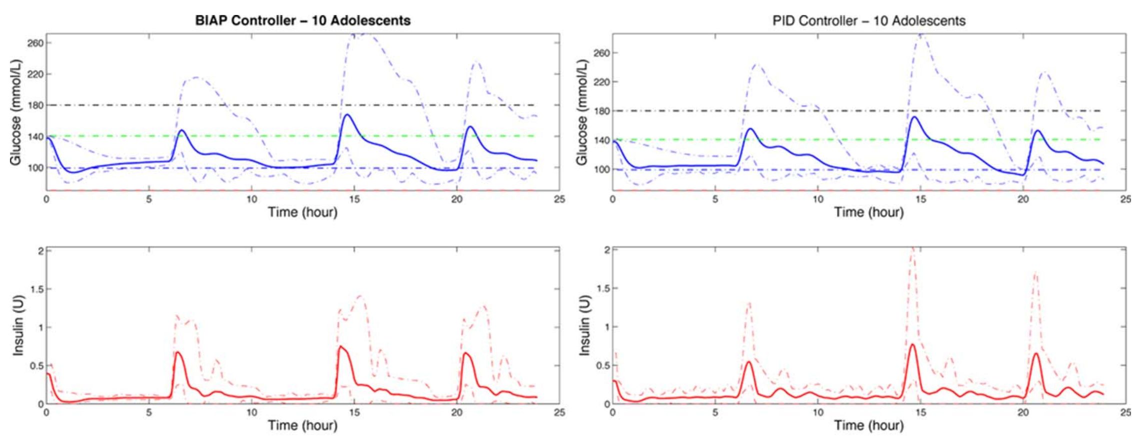

(a) (b)

Fig. 11. ePID vs. BIAP in 10 adolescents. Solid lines represents mean glucose concentration and mean insulin delivery. Dashed lines represent the envelopes containing all the curves. Breakfast, lunch and dinner occur at 6, 14 and 21 hour, respectively. (a) BIAP. (b) ePID.

selected glucose target range corresponds to the normoglycemic post-prandial glucose range in healthy subjects.

Both controllers were tested using a 24-hour scenario with an initial blood glucose of 140 mg/dl and containing 3 meals of 40 g, 60 g and 50 g of carbohydrates at times 6 am, 2 pm and 8 pm. Controller gains K (BIAP) and K_p (PID) were adjusted per subject in order to minimise hyperglycaemia and to avoid dropping below 80 mg/dl. Since only one parameter per controller was allowed to be individually tuned, parameters T_D and T_I were respectively fixed to 15 and 150 for all subjects. A sampling time of one minute was used for both controllers and the calculated insulin was delivered as a micro-bolus at each sampling time.

Table III shows the results for the BIAP and ePID controllers corresponding the adult population. Table IV shows the results for both controller corresponding the adolescent population. Fig. 10 shows a graphical comparison of the BIAP and ePID controllers for the adult population and Fig. 11 shows the same comparison but for the adolescent population. It is worth noting that, although moderate improvement, all metrics show superior glycemic control of BIAP with respect to ePID.

It is worth noting that, on average, the BIAP controller outperformed the ePID controller in all the metrics. In particular, the percentage of time in target for the BIAP was 97.3% in the adult population and 89% in the adolescent population, compared to 93.5% and 85% for the ePID controller in respective populations. Although these differences may not seem numerically significant, they can represent a notable improvement in terms of the reduction on the number of hypoglycaemic events.

VI. Conclusion

We presented an analogue implementation of the pancreatic β-cell model and showed its potential in controlling blood glucose *in-vivo*. The analogue implementation was implemented to faithfully recreate physiological responses seen in the β-cells. We showed it capable of achieving comparable insulin release profiles for a glucose step, ramp, staircase and meal stimuli. In a typical control scenario it could control glucose for three meals (breakfast, lunch and dinner) achieving good % time in target.

Our bio-inspired approach using the β-cell model captures quite accurately all effects seen in physiology to achieve physiological insulin delivery which has been shown to be important as it reduces both mitogenic any myogenic effects when controlling blood glucose [30]. Unlike the previous work by Steil *et al.* [16], it has been proven that a bio-inspired glucose controller based on a model of the β-cell physiology can provide equivalent, and in some cases superior, performance compared to a PID controller in the 10 adult and 10 adolescent virtual populations of the UVa-Padova simulator [15]. Moreover, as with other successful bio-inspired systems such as the cochlear [31], we can implement our system in CMOS with circuits which operate in weak inversion, providing additional advantages of low-power and minaturisation. Furthermore, our bio-inspired method allows a more natural extension to developing a bi-hormonal system [32], as is seen in physiology, by incorporating additional models of pancreatic cells such as the alpha cell which have been shown to be important for glucagon release, a counter regulatory hormone to insulin which can prevent hypoglycemia [33].

The analogue implementation of the system in CMOS was optimized to achieve a power consumption of 1.907 mW. This was mainly due to the large number of comparators required to recreate a bio-realstic profile by keeping the glucose step at 1 mg/dl. Applying sampled data techniques to cycle and thus re-use common blocks would greatly minimise this and is subject to further work. Furthermore techniques of designing long-time constant g_m-C filters [34] which can use on chip capacitors are promising for a future implementation of the proposed circuit on a chip. We also envisage that an analogue implementation such as this could act as a tool for better understanding and simulating clusters of β-cells as has been done in the past for neural systems [35] and chemical reactions [36]. Though the current system is limited to *in vivo* use, with the future trend of implantable glucose sensors and rapidly acting insulin we envisage that it could be applied in the future for an implantable artificial pancreas. For current subcutaneous systems the algorithm has been adopted to work [6] creating a wearable bio-inspired artificial pancreas. This will ultimately lead to better control of blood glucose and impact on diabetes management, reducing complications and improving quality of life.

REFERENCES

[1] "The effect of intensive treatment of diabetes on the development and progression of long-term complications in insulin-dependent diabetes mellitus," *New Eng. J. Med.*, vol. 329, pp. 977–986, Sep. 1993, The Diabetes Control and Complications Trial Research Group.

[2] R. Hovorka, "Closed-loop insulin delivery: From bench to clinical practice," *Nature Rev. Endocrinol.*, vol. 7, no. 7, pp. 385–395, 2011.

[3] H. Broekhuyse, H. Nelson, B. Zinman, and A. Albisser, "Comparison of algorithms for the closed-loop control of blood glucose using the artificial beta cell," *IEEE Trans. Biomed. Eng.*, no. 10, pp. 678–687, 1981.

[4] "JDRF randomized clinical trial to assess the efficacy of real-time continuous glucose monitoring in the management of type 1 diabetes: Research design and methods," *Diabetes Technol. Ther.*, vol. 4, no. 10, pp. 310–21, 2008.

[5] T. Elasy, "Insulin pumps," *Clin. Diabetes*, vol. 2, no. 25, pp. 41–42, 2007.

[6] P. Herrero, P. Georgiou, N. Oliver, D. Johnston, and C. Toumazou, "A bio-inspired glucose controller based on pancreatic β-cell physiology," *J. Diabetes Sci. Technol.*, vol. 6, no. 3, pp. 606–606, 2012.

[7] G. M. Steil, C. C. Palerm, N. Kurtz, G. Voskanyan, A. Roy, S. Paz, and F. R. Kandeel, "The effect of insulin feedback on closed loop glucose control," *J. Clin. Endocrinol. Metab.*, vol. 5, no. 96, pp. 1402–8, 2011.

[8] E. Renard, J. Place, M. Cantwell, H. Chevassus, and C. C. Palerm, "Closed-loop insulin delivery using a subcutaneous glucose sensor and intraperitoneal insulin delivery feasibility study testing a new model for the artificial pancreas," *Diabetes Care*, vol. 33, no. 1, pp. 121–127, 2010.

[9] A. Liebl, R. Hoogma, E. Renard, P. H. L. M. Geelhoed-Duijvestijn, E. Klein, J. Diglas, L. Kessler, V. Melki, P. Diem, J.-M. Brun, P. Schaepelynck-Bélicar, and T. Frei, "A reduction in severe hypoglycaemia in type 1 diabetes in a randomized crossover study of continuous intraperitoneal compared with subcutaneous insulin infusion," *Diabetes, Obesity, Metab.*, vol. 11, no. 11, pp. 1001–1008, 2009.

[10] A. Krasner, R. Pohl, P. Simms, P. Pichotta, R. Hauser, and E. De Souza, "A review of a family of ultra-rapid-acting insulins: Formulation development," *J. Diabetes Sci. Technol.*, vol. 6, no. 4, pp. 786–786, 2012.

[11] Y. M. Luijf, J. K. Mader, W. Doll, T. Pieber, A. Farret, J. Place, E. Renard, A. F. D. Bruttomesso, A. Avogaro, S. Arnolds, C. Benesch, L. Heinemann, and J. H. DeVries, "Accuracy and reliability of continuous glucose monitoring systems: A head-to-head comparison," *Diabetes Technol. Therap.*, vol. 15, no. 8, pp. 721–726, 2013.

[12] E. Johannessen *et al.*, "Toward an injectable continuous osmotic glucose sensor," *J. Diabetes Sci. Technol.*, vol. 4, no. 4, pp. 882–882, 2010.

[13] P. Georgiou and C. Toumazou, "A silicon pancreatic beta cell for diabetes," *IEEE Trans. Biomed. Circuits Syst.*, vol. 1, no. 1, pp. 39–49, 2007.

[14] P. Georgiou and C. Toumazou, "Semiconductors for early detection and therapy," *Electron. Lett.*, vol. 47, no. 26, pp. 4–6, 2011.

[15] B. P. Kovatchev, M. Breton, C. D. Man, and C. Cobelli, "In silico preclinical trials: A proof of concept in closed-loop control of type 1 diabetes," *J. Diabetes Sci. Technol.*, vol. 1, no. 3, pp. 44–55, 2009.

[16] G. M. Steil, A. E. Panteleon, and K. Rebrin, "Closed-loop insulin delivery: The path to physiological glucose control," *Adv. Drug. Deliv. Rev.*, vol. 2, no. 56, pp. 125–44, 2004.

[17] E. Breda, G. Toffolo, K. S. Polonsky, and C. Cobelli, "Insulin release in impaired glucose tolerance: Oral minimal model predicts normal sensitivity to glucose but defective response times," *Diabetes*, vol. 1, no. 51, pp. S227–33, 2002.

[18] M. G. Pedersen, R. Bertram, and A. Sherman, "Intra- and inter-islet synchronization of metabolically driven insulin secretion," *Biophys. J.*, vol. 1, no. 3, pp. 107–19, 2005.

[19] A. Bertuzzi, S. Salinari, and G. Mingrone, "Insulin granule trafficking in beta-cells: Mathematical model of glucose-induced insulin secretion," *Amer. J. Physiol. Endocrinol. Metab.*, vol. 1, no. 293, pp. E396–409, 2007.

[20] Y. Chen, S. Wang, and A. Sherman, "Identifying the targets of the amplifying pathway for insulin secretion in pancreatic ?-cells by kinetic modeling of granule exocytosis," *Biophys. J.*, vol. 5, no. 95, pp. 2226–41, 2008.

[21] M. G. Pedersen, G. M. Toffolo, and C. Cobelli, "Cellular modeling: Insight into oral minimal models of insulin secretion," *Amer. J. Physiol. Endocrinol. Metab.*, vol. 3, no. 298, pp. E597–601, 2010.

[22] R. Hovorka, L. Chassin, S. D. Luzio, R. Playle, and D. R. Owens, "Pancreatic β-cell responsiveness during meal tolerance test: Model assessment in normal subjects and subjects with newly diagnosed non-insulin-dependent diabetes mellitus," *J. Clin. Endocrinol. Metab.*, vol. 3, no. 83, pp. 744–50, 1998.

[23] G. Toffolo, E. Breda, M. K. Cavaghan, D. A. Ehrmann, K. S. Polonsky, and C. Cobelli, "Quantitative indexes of $beta$-cell function during graded up and down glucose infusion from c-peptide minimal models," *Amer. J. Physiol. Endocrinol. Metab.*, vol. 1, no. 280, pp. E2–10, 2001.

[24] A. Cretti, M. Lehtovirta, E. Bonora, B. Brunato, M. G. Zenti, F. Tosi, M. Caputo, B. Caruso, L. C. Groop, M. Muggeo, and R. C. Bonadonna, "Assessment of $beta$-cell function during the oral glucose tolerance test by a minimal model of insulin secretion," *Eur. J. Clin. Invest.*, vol. 5, no. 31, pp. 405–16, 2001.

[25] A. Mari, O. Schmitz, A. Gastaldelli, T. Oestergaard, B. Nyholm, and E. Ferrannini, "Meal and oral glucose tests for assessment of β-cell function: Modeling analysis in normal subjects," *Amer. J. Physiol. Endocrinol. Metab.*, vol. 6, no. 283, pp. E1159–66, 2002.

[26] E. M. Drakakis, A. J. Payne, and C. Toumazou, ""Log-domain state-space": A systematic transistor-level approach for log-domain filtering," *IEEE Trans. Circuits Syst. II, Analog Digit. Signal Process.*, vol. 46, no. 3, pp. 290–305, 1999.

[27] K. I. Papadimitriou and E. M. Drakakis, "CMOS weak-inversion log-domain glycolytic oscillator: A cytomimetic circuit example," *Int. J. Circuit Theory Appl.*, pp. N/a–N/a, Sep. 2012.

[28] H. Lee, B. Buckingham, D. M. Wilson, and B. W. Bequette, "A closed-loop artificial pancreas using model predictive control and a sliding meal size estimator," *J. Diabetes Sci. Technol.*, vol. 3, no. 5, pp. 1082–1090, 2009.

[29] P. Soru, G. D. Nicolao, C. Toffanina, C. Dalla-Man, C. Cobelli, and L. Magni, "MPC based artificial pancreas: Strategies for individualization and meal compensation," *Annu. Rev. Control*, vol. 36, pp. 118–128, 2009.

[30] G. Steil and G. Grodsky, "The artificial pancreas: Is it important to understand how the $beta$-cell controls blood glucose?," *J. Diabetes Sci. Technol.*, vol. 7, no. 5, pp. 941–951, 2013.

[31] J. Georgiou and C. Toumazou, "A 126-μw cochlear chip for a totally implantable system," *IEEE J. Solid-State Circuits*, vol. 40, no. 2, pp. 430–443, 2005.

[32] P. Herrero, P. Georgiou, N. Oliver, and C. Toumazou, "A composite model of glucagon-glucose dynamics for in silico testing of bihormonal glucose controllers," *J. Diabetes Sci. Technol.*, vol. 7, no. 4, pp. 941–951, 2013.

[33] F. El-Khatib, S. Russell, D. Nathan, R. Sutherlin, and E. Damiano, "A bihormonal closed-loop artificial pancreas for type 1 diabetes," *J. Diabetes Sci. Technol.*, vol. 2, no. 27, p. 27ra27, 2010.

[34] R. Rieger, A. Demosthenous, and J. Taylor, "Continuously tunable, very long time constant CMOS integrator for a neural recording implant," in *Proc. 29th Eur. Solid-State Circuits Conf.*, 2003, pp. 441–444.

[35] T. Yu and G. Cauwenberghs, "Analog vlsi biophysical neurons and synapses with programmable membrane channel kinetics," *IEEE Trans. Biomed. Circuits Syst.*, vol. 4, no. 3, pp. 139–148, 2010.

[36] S. Mandal and R. Sarpeshkar, "Log-domain circuit models of chemical reactions," in *Proic. IEEE Int. Symp. Circuits and Systems*, 2009, pp. 2697–2700.

Ilias Pagkalos received the Dipl.Ing. degree in electrical and computer engineering from Democritus University of Thrace, Xanthi, Greece, and the M.Sc. degree in analogue and digital integrated circuit design from the Department. of Electrical and Electronic Engineering of Imperial College London (ICL), London, U.K., in 2011 and 2012, respectively.

Since 2012, he has been working toward the Ph.D. degree in the Department of Bioengineering at ICL under the supervision of Dr. Emmanuel Drakakis. His research interest focuses on the design of low power analogue electronics for biomedical applications. He is a scholar of A.G. Leventis Foundation and General Arnaoutis Foundation.

Pau Herrero received the M.Eng. degree in industrial engineering from the University of Girona, Girona, Spain, and the Ph.D. degree from the University of Angers, Angers, France, and the University of Girona in 2001 and 2006, respectively.

After receiving the Ph.D. degree, he moved to Doyle's Group in the Chemical Engineering Department of University of California, Santa Barbara, Santa Barbara, CA, USA, where he spent one year as a Postdoctoral Research Fellow working on an artificial pancreas project in collaboration with Sansum Diabetes Research Institute, Santa Barbara, CA, USA. He then spent the following two years at Hospital de Sant Pau, Barcelona, Spain, working as a Research Fellow for the Biomedical Research Networking Center in bioengineering, biomaterials and manomedicine (CIBER-BBN), leading different eHealth projects for the prevention of Type 2 diabetes and management of Type 1 diabetes. Currently, he is a Research Fellow within the Centre for Bio-Inspired Technology in the Department of Electrical and Electronic Engineering, Imperial College London, London, U.K. His main research interest lies in the field of diabetes technology and in particular in developing algorithms for the realization of a bio-inspired artificial pancreas. He is also involved in the ongoing research in the development of a decision support system for Type 1 diabetes management based on case-based reasoning (CBR) technology. In addition, he is involved in a research project that aims to optimize antibiotic prescribing in the intensive care unit by providing prescribing decision support through CBR technology.

Christofer Toumazou (M'87–SM'99–F'01) received the B.Sc. degree in engineering and the Ph.D. degree in electrical engineering from Oxford Brookes University, Oxford, U.K.

He is the Founding Director and Chief Scientist of the Institute of Biomedical Engineering at Imperial College London, London, U.K., Research Director of the Centre for Bio-Inspired Technology, and the Winston Wong Chair in Biomedical Circuits in the Department of Electrical and Electronic Engineering. His research interests include high-frequency analog integrated circuit design for RF electronics and lowpower electronics for biomedical applications. He has authored more than 700 research papers and holds 40 patents in the field of semiconductors and healthcare, many of which are now fully granted PCT.

Prof. Toumazou was the Chairman of the Analog Signal Processing Committee and the Vice President of Technical Activities for the IEEE Circuits and Systems Society. He founded the IEEE Biomedical Circuits and Systems Society in 2000. He is also the Founder of technology-based companies with applications spanning ultralow-power mobile technology and wireless glucose monitors. He is a Fellow of the Royal Society, the Royal Academy of Engineering, and the Institution of Electrical Engineers. He is also a Chartered Engineer, U.K. He received the Royal Academy of Engineering Silver Medal in 2007 for pioneering contributions to British industry. In 2008, he was appointed the Fellowship of the Royal Academy of Engineering and the Fellowship of the Royal Society. In 2009, he received the World Technology Award sponsored by Time Magazine for the Health and Medicine category, followed by the 2011 J. J. Thomson Medal of the IET. In 2013, he was made a Fellow of the Academy of Medical Sciences and was conferred the title of Regius Professor during the Queens 2012 Diamond Jubilee.

Pantelis Georgiou (AM'05–M'08–SM'13) received the M.Eng. degree in electrical and electronic engineering and the Ph.D. degree from Imperial College London (ICL), London, U.K., in 2004 and 2008, respectively.

Currently, he is a lecturer within the Department of Electrical and Electronic Engineering. He is also the head of the Bio-inspired Metabolic Technology Laboratory in the Centre for Bio-Inspired Technology and part of the Medical Engineering Solutions in Osteoarthritis Centre of Excellence. His research includes bio-inspired circuits and systems, CMOS based lab-on-chip technologies, and application of microelectronic technology to create novel medical devices. He conducted pioneering work on the silicon beta cell and is now leading the project forward to the development of the first bio-inspired artificial pancreas for Type I diabetes.

Dr. Georgiou was awarded the IET Mike Sergeant medal of outstanding contribution to engineering in 2013. He is a member of the IET and serves on the BioCAS and Sensory Systems technical committees of the IEEE CAS Society. He also serves on the IET Prizes and Awards committee.